Citrus limetta based Silver Nanoparticles and their Antioxidant, Antibacterial and Biofilm Inhibition Potential

Naseem Akhter[1], Tahreem Riaz[1], Asma Yaqoob[2], Muhammad Shahid[3], Shahina Mailk[1], Musarat Batool[1]

[1]Chemistry Department, Sadiq College Women University Bahawalpur, 63100, Pakistan
[2]Institute of Biochemistry and Biotechnology, The Islamia University of Bahawalpur, 63100, Pakistan
[3]Department of Biochemistry, University of Agriculture, Faisal Abad, 38000, Pakistan

Abstract This work represents a new, cheap precursor designed for the biosynthesis of silver nanoparticles (ClAgNPs) through *Citrus limetta* leaves. The fabricated particles were analyzed by UV, FTIR, SEM, and XRD. The synthesized particles have maximum absorption at 495 nm in UV with an average size of 70 nanometres. They have shown 620.42 mg GAE/ml TPC, 129.34 mg CE/g TFC, 81.07% DPPH inhibition assay, effective antibacterial against *S. aureus* and *E. coli* with 10 and 5 mm zone of inhibition, effective biofilm in- inhibitor against S. aureus (41.55 % inhibition). The synthesized ClAgNPs have higher TPC, TFC, antioxidant, antibacterial, and biofilm potential than its Cl leaves.

Keywords

Citrus limetta; silver nanoparticles; TPC; TFC; antioxidant; antibacterial; biofilm inhibition assay

Introduction

Recently, Nanotechnology has become most impactful in all disciplines of science. It mainly focused on nanoparticle synthesis and its modification (Singh et al., 2016). In this field, the development of rapid, simple, cheap, and ecologically friendly methodologies for the synthesis of nanoparticles is (NPs) getting more attention (Hano and Abbasi, 2021). Chemical, physical, mechanical, and biological methods are different approaches used to synthesize NPs (Saha et al., 2017). The synthesis employing a chemical approach results in harmful chemical adsorption on of NPs surface, which could cause negative medical consequences. Bioinspired nanoparticle synthesis offers a cost-effective and environmentally sustainable alternative to chemical and physical approaches (Rao and Gan, 2015). This approach implies choosing an appropriate solvent, an environmentally safer reducing agent, and safer chemicals for nanoparticle stability (Geraldes et al., 2016)

Plant extracts afford a large number of secondary metabolites and biomolecules that can reduce and cape the metal ion to a metal nanoparticle, respectively (Alloosh et al., 2021). The genus *Citrus* belongs to the Rutaceae family known as the orange family having 120 genera and 900 species. The antiseptic and antibacterial properties of sweet lime make it an ideal choice for combating infections, ulcers, and wounds. This property of said specie can enhance the blood circulatory and immune system and the body can better fights against cancer (Yi et al., 2017)

The Mosambi is known as sweet lime also. It is grown extensively in Asia (Hashemi et al., 2017; Shakoor and Nasar, 2016). This specie has a high concentration of flavonoids, phenolic acid, volatile terpenoids, amino acids, and vitamin C which are effective cancer-fighting agents (Kundu and Banerjee, 2020). These constituents offer a broad spectrum of antimicrobial anticancer and anti-diabetic potential and perform a defensive role against pathogens. They can alter enzyme action in the body, decrease the chance of malignant cell division and act as antioxidants (Kumar et al., 2022).

Silver is a very well disinfectant that can kill microbes over a wide range, including bacteria, fungi, and viruses. Sine time, silver was used in the treatment of multiple diseases in medical systems (Mohamed, Abd El-Baky, Sandle, Mandour, & Ahmed, 2020). In history, silver nitrate drops were used to disinfect infants' eyes from Neis- seria gonorrhea infection (Pryjmakova et al., 2020). This metal is the most potent among all antibacterial metals (Gugala et al., 2017). This activity of silver is used in medicine for the treatment of bacterial colonization on artificial body parts, body tubes, and tissues, dental surgery materials, and human skin, as well as burn therapy and arthroplasty (Pryjmakova et al., 2020)

Bacteria cells grow in colonies in 3-dimensional patterns making biofilm structures (Chong et al., 2019). These Biofilms are embedded on the surface of polymeric materials (Catto and Cappitelli, 2019) cause antibiotics ineffectiveness, which is a challenge to clinical and pharmaceutical researchers (Li and Webster, 2018). In addition, biofilm formation also leads to economic loss (Arunkumar et al., 2020) to the industries due to corrosion, loss of heat transfer, and increase in friction.

Currently, designed for the production of ClAgNPs by means of an aqueous *C. limetta* leaf extract (Mosambi), on which no work was found previously. In the present work, the leaf of mosambi extract resulted in a significant synthesis of ClAgNPs. SEM, FTIR and XRD and UV-VIS techniques applied to determine the size, morphologies charge of the nanoparticles. Synthesized ClAgNPs were tested against antibacterial, antioxidant, and biofilm inhibition potential

Material and Methods

General Chemicals

Analytically rated and Sigma Aldrich labelled chemicals employed in the current in- vestigation.

Plant Collection

Citrus limetta leaves were collected from the lawn of my house located in Bahawalpur, Pakistan in October 2020 and identified by the Botany Department, Govt. Sadiq College Women University Bahawalpur
(GSCWU).

General Procedure for Bio-Synthesis of Silver Nanoparticles

Leaves of *Citrus limetta* (Cl) were washed shade dried and chopped into fine pieces. 20g of finely chopped leaves were soaked in boiled distilled water 50ml for 20 minutes. Upon cooling the solution, filtration was performed by Whatman filter paper no. 41. For further use Cl extract was refrigerate at 4 ^{0}C. The silver nitrate solution (0.5mM) was prepared. 45 ml of silver solution and 5 ml of Cl extract were mixed and incubated for 2.5 hours for the temporal changes. The solution became brown indicating the formation of ClAgNPs. The synthesized particles were dispersed in distilled water and subjected to centrifugation at 12000 rpm for 15 minutes. The synthesized ClAgNPs were filtered, washed, and dried at a temperature of 60^{0}C (Figure 1).

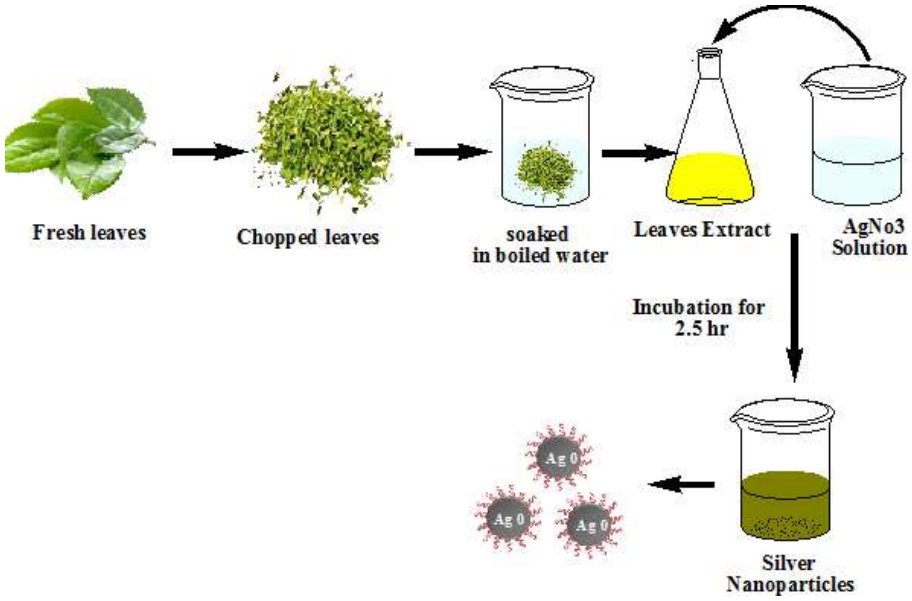

Fig. 1 Protocol for the synthesis of ClAgNPs using *Citrus limetta*

Silver Nanoparticles Characterization

The ClAgNPs formation was preliminary verified by Agilent Cary 60 UV Visi- ble spec- trophotometer (UV visible), The functionalities accountable for biore- duction and stabilization were analyzed using 80R-FTIR Agilent Cary 630Fourier Transforms Infrared spectroscopy (FTIR), and the physical features and morphology of synthesized particle were studied by Nova NanoSEM 450 field emission scanning electron microscope (FE-SEM), The composition of ClAgNP was determined by using EDX (EDX integrated with FE-SEM). The crystallinity and crystal size were determined using D2 Phaser Bruker X-ray diffraction (XRD).

Determination of Phenolic Contents

The phenolic content of methanolic plant extract was measured by using the Folin Ciocalteu technique described in (Cicco et al., 2009). By combining gallic acid solution in methanol, 0.01, 0.02, 0.03, 0.04, 0.05, 0.06, 0.07, 0.08 ,0.09, and 0.10 mg/mL, 4 mL of sodium carbonate (20%) and 5 mL of tenfold diluted Folin-Ciocalteu reagent the calibration curve was created. The absorbance at 765nm was measured by plotting absorbance as a function of concentration after just one hour to create the calibration curve. The same reagent as stated above was combined with 1mL of plant extract (0.001g/mL), and the absorbance of the resultant blue colour complex was measured at 765nm after approximately one hour. Each judgment was made three times. Measurement of the standard was done (gallic acid). The total phenolic compounds in plant extracts was estimated as gallic acid equivalents (GAE) by using the formula T = C x V / M.

Where V is extract's volume in milliliters, T is the total amount of phenolic compounds, M is its weight in grams measured in milligrams of GAE per kilogram of plant extract, and C is the gallic acid concentration, measured in milligrams per milliliter using the calibration curve.

Determination of Flavonoid Contents

In plant extracts, overall flavonoid content material is measured by the use of the technique described in (Rehman et al., 2013). Shortly after, 0.5 mL of plant extract was incubated for six minutes with 0.15 mL of 5% $NaNO_2$ and 2 ml of distilled water. Subsequently 0.15mL of 10% $AlCl_3$ solution delivered and the mixture changed into incubated for six minutes before being handled with 4% NaOH solution. Including methanol in the reaction mixture the volume of mixture expanded to 5ml. of incubation, the absorbance of the reaction combination became dignified at 510nm after 15 minutes (Ayub et al., 2017). The extract's TFC expressed as catechin equivalents in step per mL of plant extract.

Antioxidant Activity Assessment

The radical scavenging potential of plant extracts turned into evaluated the usage of the 2,2-diphenyl-1-picrylhydrazyl (DPPH) (Siddiqui et al., 2020). 1mL from 0.004 percentage DPPH in methanol solution (freshly produced) was added to plant extract (3ml) and the combined solution was maintained in the dark. At 517 nm absorbance change is measured. A reaction aggregate with a low absorbance has a sturdy radical scavenging interest. The antioxidant pastime of BHT and ascorbic acid become additionally investigated. As a control, a solution lacking plant extract became obtained (Naseem et al., 2020). All experiments have been carried out in duplicate. As a positive control, ascorbic acid was employed.

DPPH percentage inhibition was calculated as follows.

DPPH Inhibition (%) = Blank absorbance (A_0 – Sample absorbance (A_1)*100 Blank absorbance (A_0)

Where A_0 = Absorbance of the blank A_1 = Absorbance of the sample..

Antibacterial Activity

Individual samples were examined against bacterial traces, inclusive of Gram- superb *Staphylococcus aureus (S.aureus)* and Gram-terrible *Escherichia coli (E. coli)*. The Institute of Microbiology, Agriculture University Faisalabad Pakistan, confirmed the purity and identity of the samples. Bacterial strains had

been grown in Nutrient agar overnight at 37 ^{0}C (Oxoid, UK). The compounds' super antibacterial activity was tested by using the disc diffusion approach. 100 L of tested microorganism suspension comprised on nutrient agar medium 107 colony-forming devices of bacteria cells. Individually impregnated with a chemical solution, the filter discs had been put on agar plates formerly inflamed with tested microorganism. As a negative control, discs without samples were utilized. (30 g/dish) For comparing the sensitivity of strain in analyzed bacterial species, rifampicin (Oxoid, UK) became utilized as a wonderful reference for microorganisms. Plates had been incubated at
37 ^{0}C for 18 hours following 2 hours at 4 ^{0}C. The antibacterial activity of the organisms was analyzed by the measurement of the width of the growth inhibition zones (region reader)

Biofilm Inhibition

Sterilized plain plastic tissue cultivation plate was loaded with 100 L of dietary broth and 20 L of injectable bacterial solution (Oxoid, UK), and 100 L of the test sample. Within the poor control wells, nutrient broth essentially became the only thing. The plates were added, and they underwent a 24-hour aerobic incubation at 37 C. The contents of each well had undergone three rinses in 220 L of sterile phosphate buffer. The plates have undergone a vigorous shaking procedure to get rid of any non-adherent microorganisms. The ultimate adhering microorganism was constant the use of 99 % methanol 220 microliters, and the plates have been emptied and allowed to dry after 15 minutes. After that, 220 mL of 50% crystal violet was placed in each well of the plates to stain them for five minutes. The dish was washed under running water to get rid of the extra stain. The dye that was adhered to the adherent cells was once again solubilized using 220 L of 33% (v/v) glacial acetic acid in each well after the plates had been air-dried. Using a microplate reader (BioTek, USA), each well's optical density (OD) at 630 nm is precisely measured (Qasim et al., 2020). Every bacterial strain has been examined three times, with the results being averaged. The percentage of inhibition of bacterial growth (INH%) was calculated using the following formula:

$$INH\ \% = 100 - (OD_{630sample} * 100) / OD_{630control}$$

Results and Discussion

UV Visible and FTIR Analysis

The ClAgNPs formation was firstly analyzed in the laboratory by UV-Visible spectrom- etry in the range of 390-550 nm. The absorption band revealed the successful reduction of Ag+ ion to Ag NPs using leaf extracts of *Citrus limetta*. The λ^{max} was observed in the range of 490 nm (Figure 2).

The FTIR of ClAgNPs has prominent absorption peaks at vibration frequencies of 3400 2000, 1627, 1394, 1088-1127, and 637 cm 1 for, C=O, OH, C-O, C-N, C=N and reduced silver. The signal is indicative of proteins involved in the bioreduction and stabilization of ClAgNPs (Figure 3). The proposed mechanism for the reduction of Ag+ to Ag^0 is shown in Figure 4.

SEM and EDX Analysis

Scanning Electron Microscope was used to examine the magnitude and surface shape of the ClAgNPs (Figure 5). The synthesized particles had average size of 70 nm, calculated from SEM histogram (Figure 6) and spherical in shape

The element composition of ClAgNPs was analyzed by EDX (Figure 7). The peak at 3 keV was represented by reduced silver metal. The other prominent element was observed for chlorine carbon and oxygen. The elements other than Ag are most likely to be obtained from the extract of leaves (Iftikhar et al., 2020).

XRD Analysis

XRD was used to find out the crystalline size and structure of the ClAgNPs manufactured by the green method. XRD diffract gram showed Bragg peaks at 2θ values of 38.75 and 44.81 attributed to planes of (111) and (200) (Figure 8). The mentioned peaks indicate that ClAgNPs are fcc and crystalline (ICDD 893722). Bragg's peaks broad- ening suggests the reduction of silver ions to nanoparticles (Singh et al.,

2021). The Debye-Scherrer equation was used to determine the average diameter of the nanoparticles D=0.94 Cos. The two Bragg peaks at 2θ values 64 and 77 mentioned in the literature (Taha et al., 2020) are not present in the XRD of ClAgNPs as this image was taken in the range 2θ value 20-60. Similar results in silver nanoparticles synthesized using Neem leaves (Taha et al., 2020).

Quantitative Phytochemical Analysis

Total Flavonoid Content and Total Phenolic Content Determination

Total phenolic contents of ClAgNPs (620.4181818 mg GAE/mL) were found greater than Cl leaves extract (542.0545455 mg GAE/mL). The results of TPC are shown in (Figure9). In the same way, ClAgNPs (129.3421053 mg CE/g) have a greater TFC content than a plant extract (Figure 10)

Antioxidant Activity by DPPH Asssay

An antioxidant assay was performed by applying DPPH scavenging activity. The ClAgNPs were found more active having higher DPPH scavenging activity (81.06977)% inhibition) than Cl leaves extract (78.83721 % inhibition) (Figure 11).

The resultant behavior was similar to TPC.

Antibacterial Activities

The ClAgNPs were subjected to antibacterial activity against two bacterial strains utilizing ciprofloxacin as a reference standard. The ClAgNPs were found more active against S. aureus than E. coli (Figure 12) showing 10mm and 5mm zone of inhibition while leave extract (Cl extract) was inactive against both strains)

Biofilm inhibition analysis

The Cl leaves extract and ClAgNPs were subjected to inhibition assay against *S. aureus* and *E. Coli*. The Cl extract showed 7.2463% inhibition against *E.Coli* while 3.86473% inhibition against *S. aureus*. In contrast, to leave extract the ClAgNPs are more vigorous against *S. aureus* than *E. Coli* with percentage inhibition of 41.5459 and 14.49276 % respectively (Figure 14).

Conclusion

Citrus Limetta derived silver nanoparticle ClAgNPs were bio-reduced and sta- bilized by proline of plant extract. This route to synthesize silver nanoparticle is a simple and eco-friendly green synthesis. The synthesized particle were of 70 nm size with circular Morphology. The ClAgNPs have higher TPC, TFC, DPPH scavenging activity, higher antibacterial active and biofilm inhibitor against S. aureus than then the pre- cursor extract. It is concluded that the synthesized particle could be good source of antioxidant and promising antibacterial and biofilm inhibitor against S. aureus.

Acknowledgment

We are thankful to ORIC (GSCWU) for financial aid

Compliance with ethical standards

No conflicts of interest have been disclosed by the authors. Appendices) tables with captions (on separate pages); figures; figure captions (as a list).

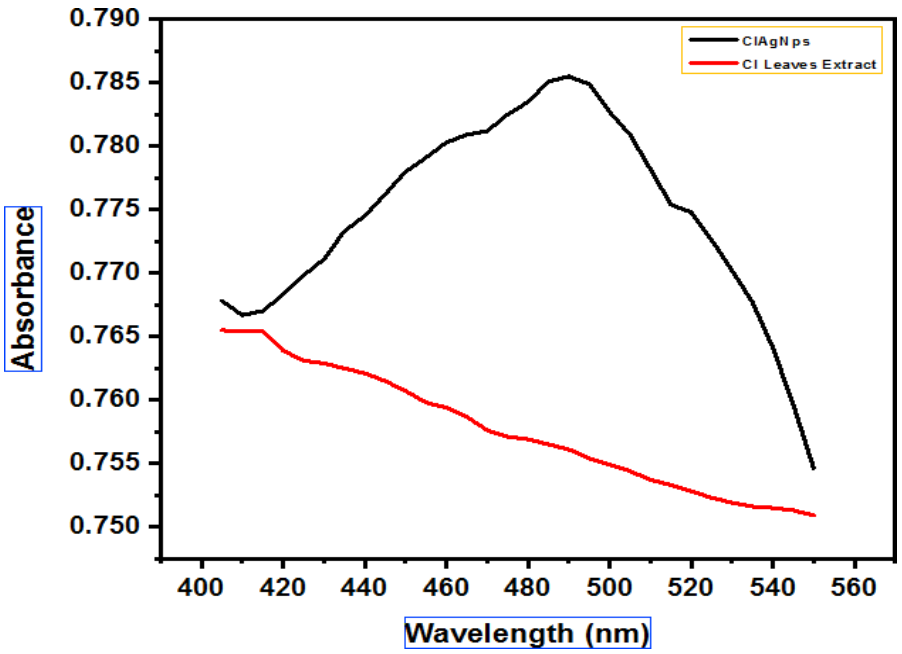

Fig. 2 UV Visible Spectrum of ClAgNPs and Cl leaves

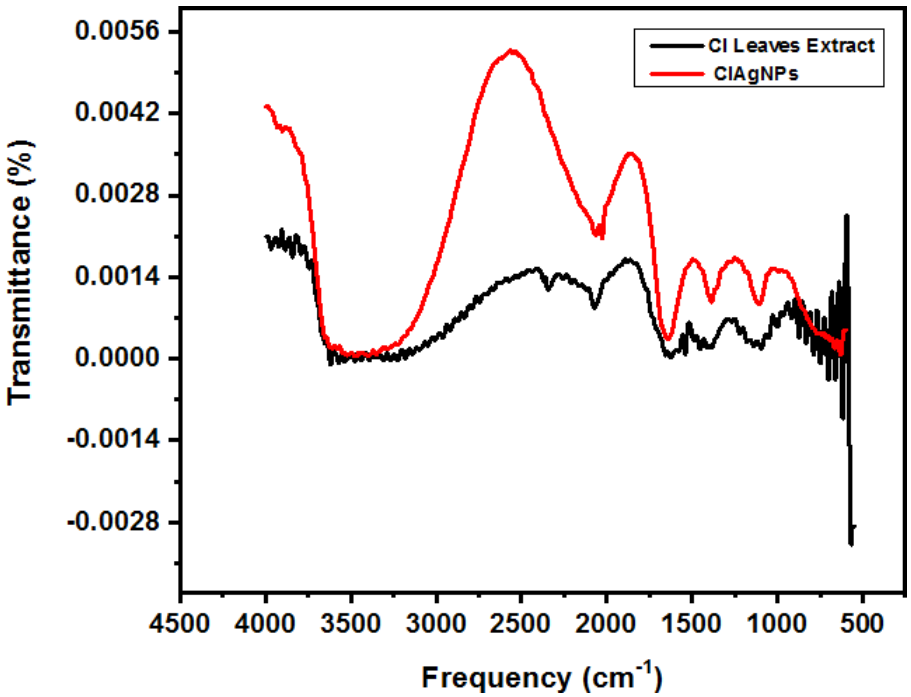

Fig. 3 FTIR of ClAgNPs and Cl leaves

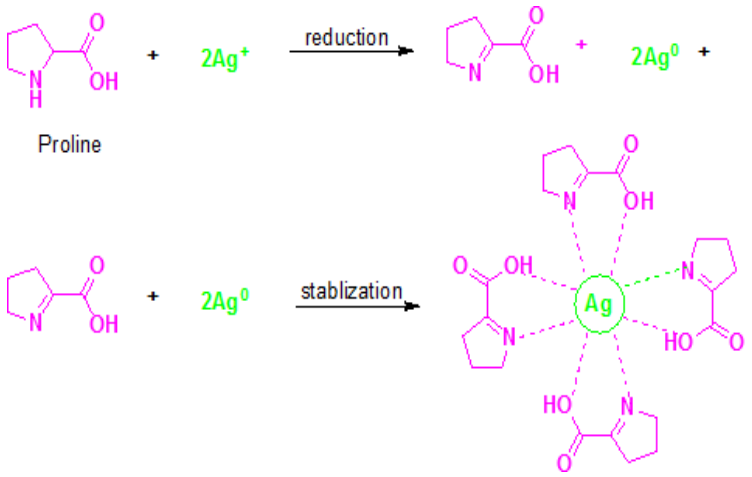

Fig. 4 Proposed Mechanism for Bioredcution of ClAgNPs

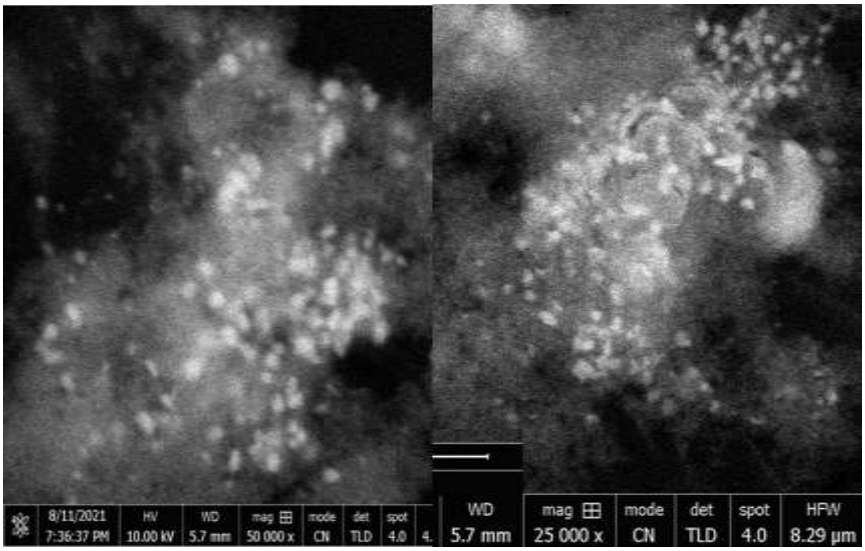

Fig. 5 SEM images of ClAgNPs

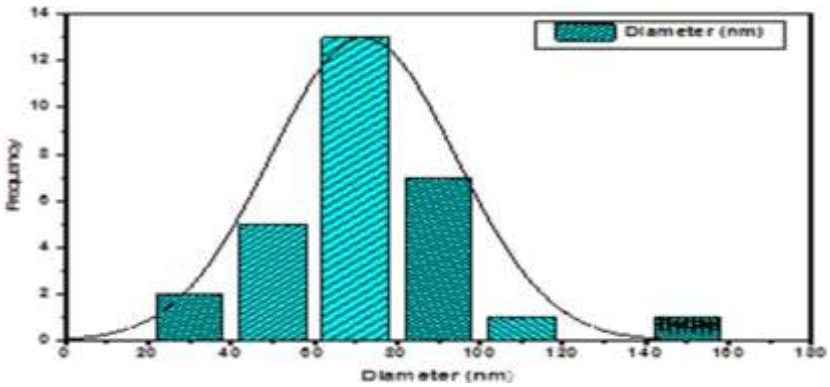

Fig. 6 SEM HistogramClAgNPs synthesized from Citrus limetta.

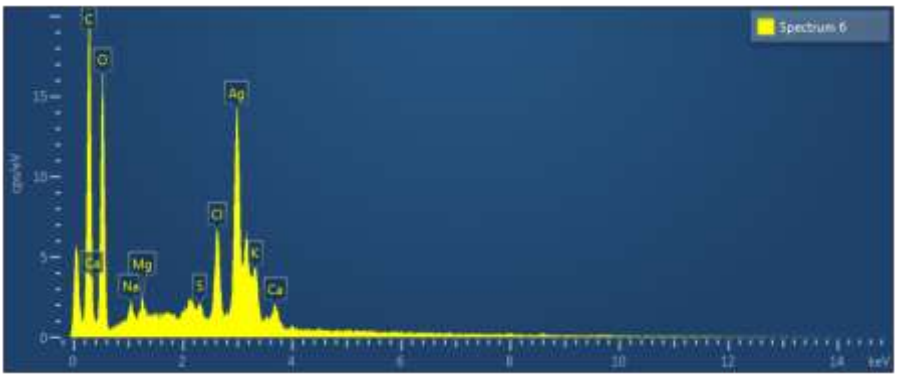

Fig. 7 EDX ClAgNPs synthesized from Citrus limetta

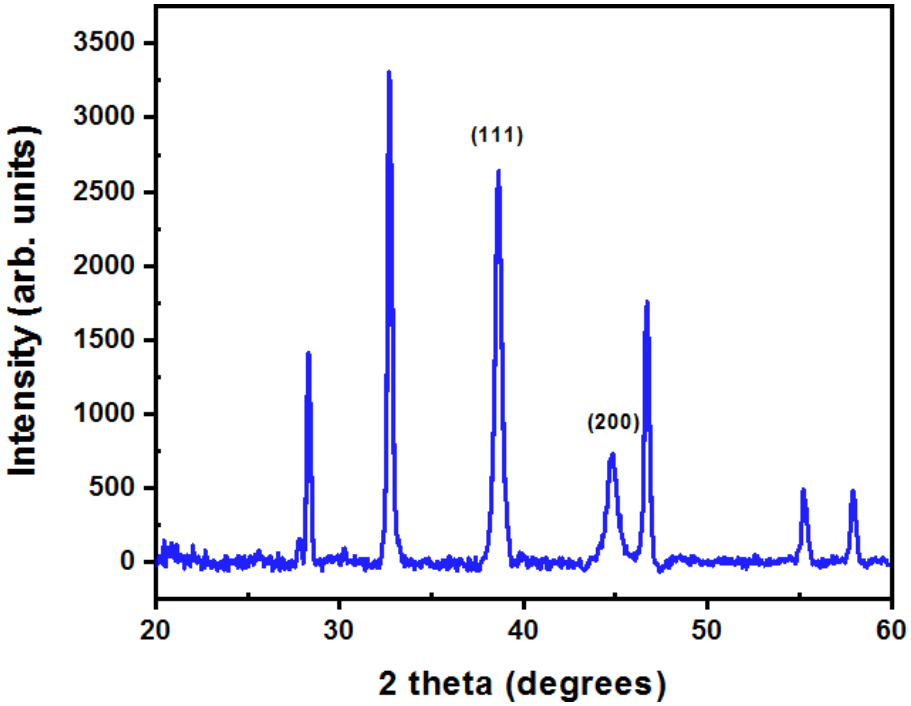

Fig. 8. XRD of Biosynthesized ClAgNPs

]

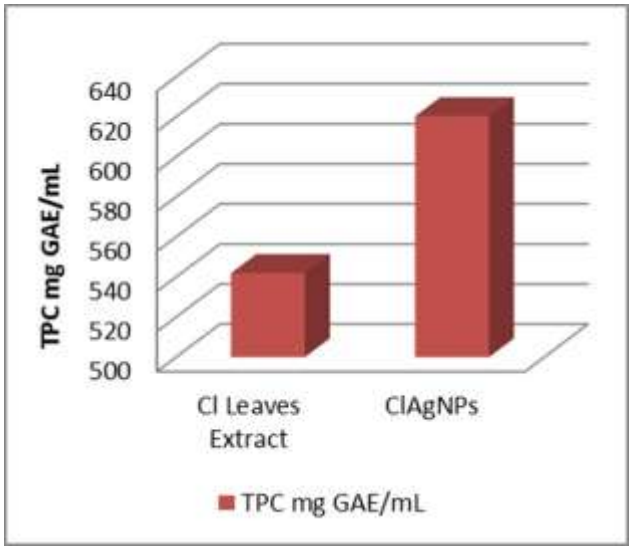

Fig. 9 Total Phenolic Contents of ClAgNPs with Cl leaves extract

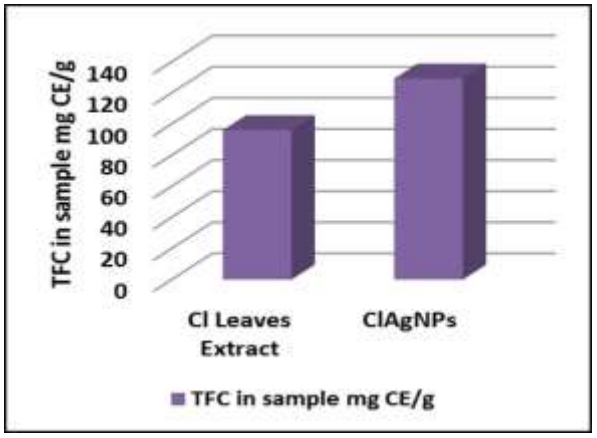

Fig. 10 Total Flavonoids Contents ClAgNPs with Cl leaves extract

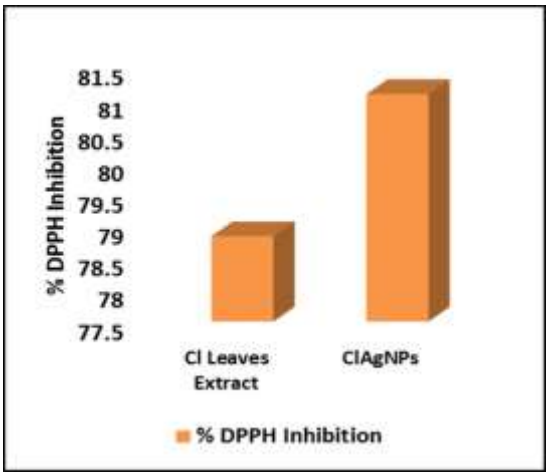

Fig. 11 Antioxidant of Cl Leaves Extract andClAgNPs

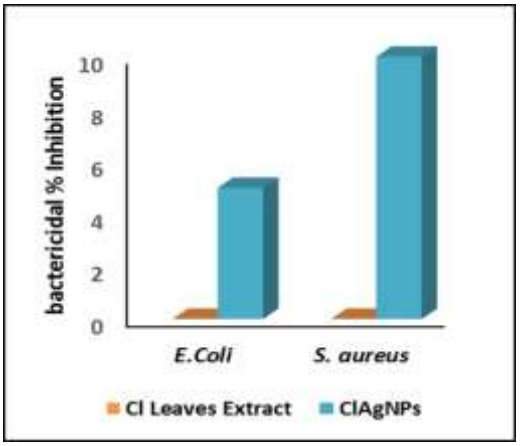

Fig. 12 Antibacterial Activity of Cl Leaves Extract andClAgNPs

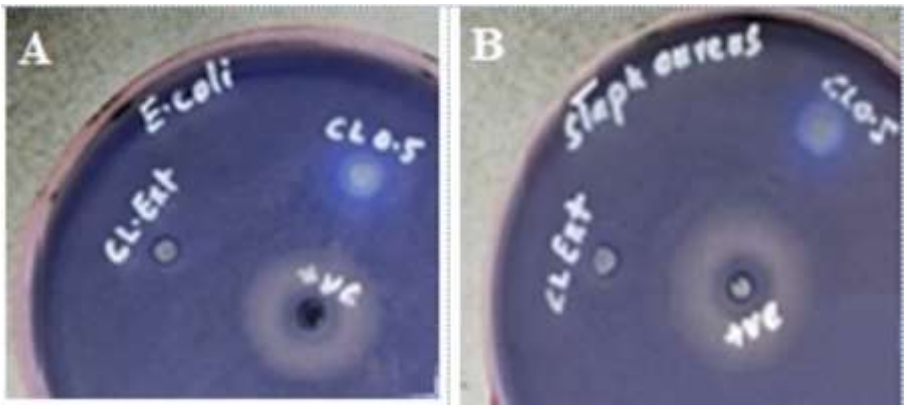

Fig. 13 Zone of Inhibition against *E.coli* (A) and *S. aureus* (B)

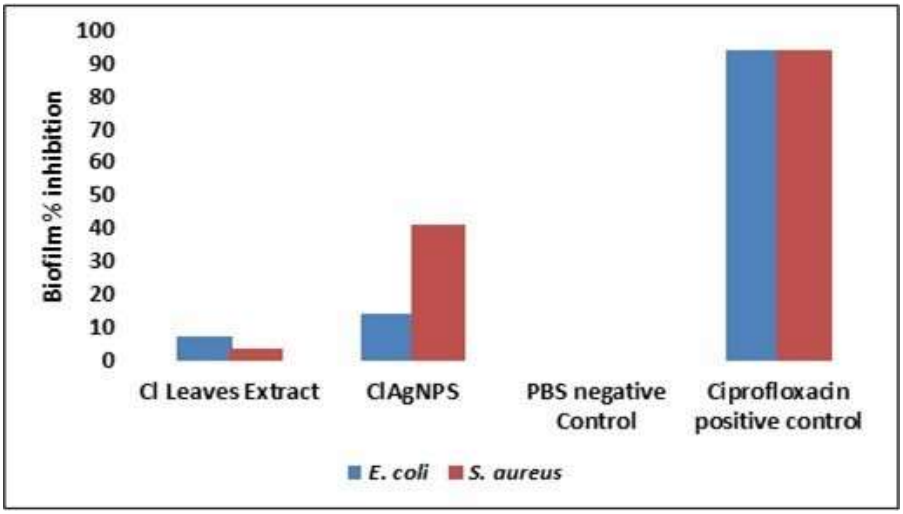

Fig. 14 Bioftlm Inhibition assay for Cl leaves Extract and ClAgNPs against E.coli and S. aureus

References

Alloosh MT, Saleh MM, Alnaddaf LM, Almuhammady AK, Salem KF, Al-Khayri JM (2021) Biosynthesis and characterization of microorganisms-derived nanomaterials. Nanobiotechnology, 239–239

Arunkumar M, Lewisoscar F, Thajuddin N, Pugazhendhi A, Nithya C (2020) vitro and in vivo biofilm forming Vibrio spp: a significant threat in aquaculture. *Process Biochemistry 94*: 213–223

Ayub MA, Hussain AI, Hanif MA, Chatha SAS, Kamal GM, Shahid M, Janneh O (2017) Variation in phenolic profile, β-Carotene and flavonoid contents, biological activities of two tagetes species from Pakistani flora. Chemistry & Biodiversity 14(6) e1600463.

Catto C, Cappitelli F (2019) Testing anti-biofilm polymeric surfaces: Where to start? International Journal of Molecular Sciences 20(15):3794–3794

Chong P, Erable B, Bergel A (2019) Effect of pore size on the current produced by 3-dimensional porous microbial anodes: A critical review. Bioresource Technology 289:121641–121641

Cicco N, Lanorte MT, Paraggio M, Viggiano M, Lattanzio V (2009) A reproducible, rapid and inexpensive Folin-Ciocalteu micro-method in determining phenolics of plant methanol extracts. Microchemical Journal 91(1):107–110

Geraldes AN, Silva AAD, Leal J, Villegas GME, Lincopan N, Katti KV, Lugao AB (2016) Green nanotechnology from plant extracts: synthesis and characterization of gold nanoparticles. Advances in Nanoparticles 5(03):176–176

Gugala NJA, Lemire RJ, Turner (2017) The efficacy of different anti-microbial metals at preventing the formation of, and eradicating bacterial biofilms of pathogenic indicator strains. The Journal 70(6)

Hano C, Abbasi BH (2021) Plant-based green synthesis of nanoparticles: production, characterization and applications. *Biomolecules 12* (1): 31–31

Hashemi SMB, Khaneghah AM, Barba FJ, Nemati Z, Shokofti SS, Al-Izadeh F (2017) Fer- mented sweet lemon juice (*Citrus limetta*) using Lactobacillus plantarum LS5: Chemical composition, antioxidant and antibacterial activities. Journal of Functional Foods 38:409– 414

Iftikhar M, Zahoor M, Naz S, Nazir N, Batiha GES, Ullah R, Mahmood, M H (2020) Green synthesis of silver nanoparticles using *Grewia optiva* leaf aqueous extract and isolated compounds as reducing agent and their biological activities. Journal of Nanomaterials

Kumar V, Kaur R, Aggarwal P, Singh G (2022) Underutilized Citrus species: An insight of their nutraceutical potential and importance for the development of functional food. Scientia Horticulturae 296:110909–110909

Li B, Webster TJ (2018) Bacteria antibiotic resistance: New challenges and opportunities for implant-associated orthopedic infections. Journal of Orthopaedic Research® 36(1):22–32

Naseem Z, Zahid M, Hanif MA, Shahid M (2020) environmentally friendly extraction of bioactive compounds from Mentha arvensis using deep eutectic solvent as green extraction media. Polish Journal of Environmental Studies 29(5):3749–3757

Pryjmakova J, Kaimlova M, Hubacek T, Svorcik V, Siegel J (2020), Nanostructured ma- terials for artificial tissue replacements. International Journal

of Molecular Sciences 21(7):2521–2521

Rao PV, Gan HS (2015) Recent advances in nanotechnology-based diagnosis and treatments of diabetes. Current Drug Metabolism 16(5):371–375

Rehman FU, Adeel S, Shahid M, Bhatti IA, Nasir F, Akhtar N, Ahmad Z (2013) Dyeing of γ-irradiated cotton with natural flavonoid dye extracted from irradiated onion shells (*Allium cepa*) powder. *Radiation Physics and Chemistry, 92*, 71-75

Saha J, Begum A, Mukherjee A, Kumar S (2017) A novel green synthesis of silver nanoparticles and their catalytic action in reduction of methylene blue dye. Sustainable Environment Research 27(5):245–250

Shakoor S, Nasar A (2016) Removal of methylene blue dye from artificially contaminated water using Citrus limetta peel waste as a very low cost adsorbent. Journal of the Taiwan Institute of Chemical Engineers 66:154–163

Siddiqui AJ, Danciu C, Ashraf SA, Moin A, Singh R, Alreshidi M, Alkhinjar MI (2020)

Singh P, Kim YJ, Zhang D, Yang DC (2016) Biological synthesis of nanoparticles from plants and microorganisms. Trends in Biotechnology 34(7):588–599

Singh R, Hano C, Nath G, Sharma B (2021) Green biosynthesis of silver nanoparticles using leaf extract of *Carissa carandas* L. and their antioxidant and antimicrobial activity against human pathogenic bacteria. Biomolecules 11(2):299–299

Taha A, Aissa MB, Dana E (2020) Green synthesis of an activated carbon-supported Ag and ZnO nanocomposite for photocatalytic degradation and its antibacterial activities. Molecules 25(7):1586–1586

Yi LS, Ma D, Ren (2017) Phytochemistry and bioactivity of Citrus flavonoids: a focus on antioxidant, anti-inflammatory, anticancer and cardiovascular protection activities. Phytochemistry Reviews 16(3):479–511

List of Figures